

# RSC Advances

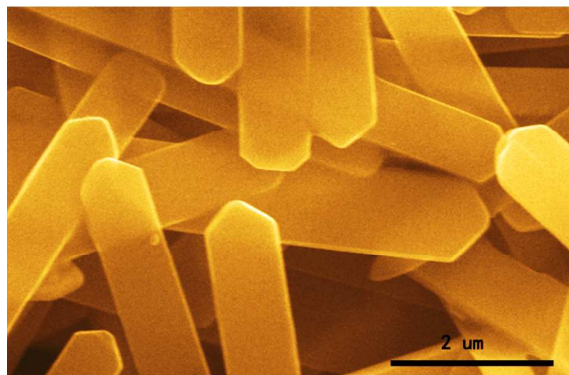


This is an *Accepted Manuscript*, which has been through the Royal Society of Chemistry peer review process and has been accepted for publication.

*Accepted Manuscripts* are published online shortly after acceptance, before technical editing, formatting and proof reading. Using this free service, authors can make their results available to the community, in citable form, before we publish the edited article. This *Accepted Manuscript* will be replaced by the edited, formatted and paginated article as soon as this is available.

You can find more information about *Accepted Manuscripts* in the [Information for Authors](#).

Please note that technical editing may introduce minor changes to the text and/or graphics, which may alter content. The journal's standard [Terms & Conditions](#) and the [Ethical guidelines](#) still apply. In no event shall the Royal Society of Chemistry be held responsible for any errors or omissions in this *Accepted Manuscript* or any consequences arising from the use of any information it contains.

**Graphical Abstract**

The elongated hexagonal  $\alpha$ -titanium phosphate nanoplates with single-crystal and controllable structures were synthesized in supercritical ethanol without any template.

## COMMUNICATION

# Supercritical Synthesis of Layered Elongated Hexagonal Titanium Phosphate Nanoplates

Cite this: DOI: 10.1039/x0xx00000x

Jiehua Liu,<sup>a\*</sup> and Xiangfeng Wei<sup>ab</sup>

Received 00th January 2012,

Accepted 00th January 2012

DOI: 10.1039/x0xx00000x

www.rsc.org/

**Well-ordered layered, elongated hexagonal  $\alpha$ -titanium phosphate ( $\alpha$ -TiP) nanoplates were synthesized in supercritical ethanol without template. The morphologies and structures of elongated hexagonal  $\alpha$ -TiP nanoplates were controlled by temperature. The possible growth mechanism of the novel  $\alpha$ -TiP structure was also proposed on the basis of powder X-ray diffraction, scanning electron microscopy, transmission electron microscope, thermogravimetric analysis, Fourier transform infrared and X-ray photoelectron spectroscopy.**

## Introduction

It is well known that supercritical fluids have been developed as environmentally benign solvents, characterized primarily by continuously adjustable physicochemical properties (for example density, viscosity, and dielectric constant, etc.) with temperature and pressure. The special physical and chemical properties of supercritical dioxide carbon<sup>1,2</sup>, supercritical water<sup>3,4</sup> and supercritical ethanol<sup>5</sup> have been extensively studied. In particular, the supercritical ethanol was one of the most popular supercritical systems for several main reasons as below. Firstly, it may offer novel media for both chemical reactions and separations as a replacement for environmentally undesirable organic solvents. Secondly, the unique solvent properties of ethanol under supercritical conditions offer possibilities to improve selectivity, enhance rate, tailor phase behaviour and facilitate separation by adjusting temperature and pressure. In addition, its critical point (241 °C, 6.14 MPa) is easier to be controlled than other supercritical fluids such as supercritical water (274.1 °C, 22.1 MPa). Although the supercritical ethanol has been applied to

many processes, its application in material science is little. Recently, with the aid of supercritical ethanol, titania/carbon nanotube composites, CeO<sub>2</sub> and graphene oxide were successfully prepared.<sup>6-8</sup>

In the past several decades, TiP, as a kind of typical metal phosphate, has been extensively studied as catalyst<sup>9,10</sup>, catalyst carrier<sup>11,12</sup>, electrochemical immunoassays<sup>13,14</sup>, molecular sieves<sup>15</sup> and ion exchanger<sup>16,17</sup>, due to well-ordered or porous frameworks, high surface area and complex forms.  $\alpha$ - and  $\gamma$ -phase TiP has been known in 1960-70s and then  $\rho$ - and  $\pi$ -phase has been reported by Bortun and coworkers.<sup>18,19</sup> Solvothermal synthesis method was applied to synthesize many new TiPs, hexagonal mesotextured titanium(IV) fluorophosphate, various titanium phosphate thin films.<sup>20,21</sup> TiP nanotubes with alternating interlayer spacing have also been prepared in H<sub>3</sub>PO<sub>4</sub>/trioctylamine/benzene microemulsion.<sup>22</sup> TiPs were synthesized and successfully used to incorporate silver ions.<sup>17,23,24</sup> In most synthesis process, the templates, including surfactants, alkyl amines and other organic molecules, are usually used to direct the formation of TiP.<sup>17,25,26</sup> More and more attention is paid on template-free method to synthesize nanoscale materials.

In this work, we proposed a facile template-free method to synthesize TiP materials in supercritical ethanol system and well-ordered elongated hexagonal TiP nanoplates were successfully obtained. By controlling the reaction conditions, the sizes of TiP materials could be tuned. Based on the experimental results, a model of the crystal growth of TiP was proposed.

## Results and discussion

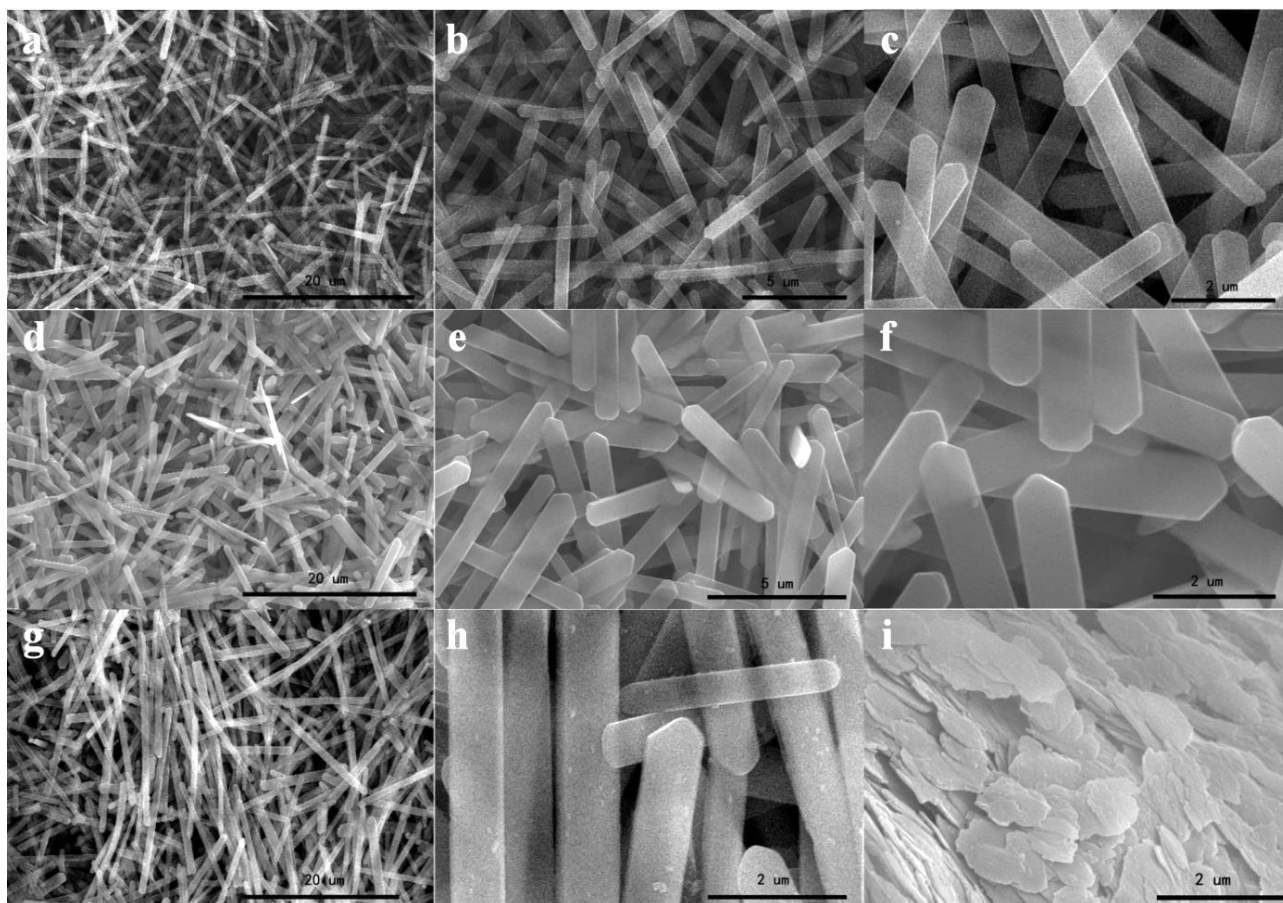


**Figure 1.** SEM images of TiP materials obtained at different conditions: (a–c) 250 °C for 5 hours, (d–f) 250 °C for 10 hours, (g and h) 270 °C for 10 hours and (i) 200 °C for 5 hours.

The morphology of the as-synthesized products synthesized at 250 °C was investigated with SEM images and the results are shown in Figure 1a–1f. It was revealed that the well-ordered nanoplates with elongated hexagonal structure were formed in supercritical ethanol at 250 °C. According to Figure 1a–1c, the elongated hexagonal  $\alpha$ -TiP nanoplates synthesized for 5 hours in supercritical ethanol system have a scale about 50–90 nm in thickness, 400–800 nm in width, and 5–11  $\mu\text{m}$  in length. With increasing the reaction time to 10 hours, there is no notable change in the size of elongated hexagonal  $\alpha$ -TiP nanoplates (shown in Figure 1d–1f), indicating that 5 hours are enough for the formation of  $\alpha$ -TiP structure. The effect of reaction temperature on the morphologies of  $\alpha$ -TiP was investigated. Figure 1g and 1h show the SEM images of  $\alpha$ -TiP synthesized at 270 °C for 10 hours, from which the well-ordered nanofibers were clearly observed. The product had a scale 60–100 nm in thickness, 500–900 nm in width, and 12–22  $\mu\text{m}$  in length. By comparison of Figure 1g and 1h with Figure 1e–1h which were synthesized at 250 °C for 10 hours, it is evident that the width and length of the elongated hexagonal  $\alpha$ -TiP nanoplates obtained at higher temperature of 270 °C are larger than those obtained at 250 °C. The products of  $\alpha$ -TiP were also prepared at the other lower temperatures of 200 °C, and the morphology is shown in Figure 1i. It is obviously found that the  $\alpha$ -TiP

nanosheets were obtained at lower temperature. The diameter obtained at 200 °C is  $700 \pm 200$  nm. Therefore, through the facile regulation of the reaction temperature, the morphologies and sizes of the  $\alpha$ -TiP framework can be controlled.

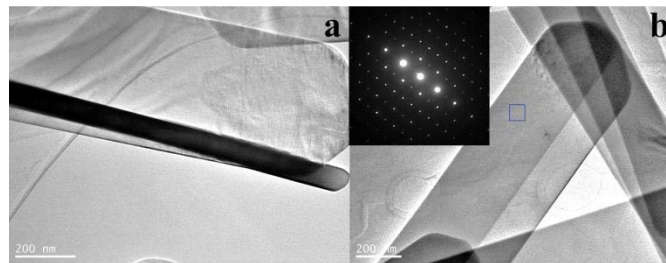


**Figure 2.** TEM images (a–b) and SEAD image obtained in square position (inset of Figure 2b) of TiP material obtained at 250 °C for 5 hours.

TEM images were provided in Figure 2. The thickness of elongated hexagonal  $\alpha$ -TiP nanoplate is  $\sim 80$  nm. The selected area electron diffraction (SEAD) image also shows the elongated nanoplate has a single-crystal structure. However, because the crystal structure is unstable at the high-resolution test condition, ordered lattices cannot be observed in HRTEM

image (Figure S1). To affirm the elemental distribution of Ti and P, STEM and elemental mapping were provided in Figure S2. Figure S2b and S2c show uniform distribution of phosphorus and titanium.

The phase structure of the as-synthesized TiP was further characterized by XRD. Figure 3a shows the XRD pattern of the product obtained in supercritical ethanol system at 250 °C for 5 hours, of which all the diffraction peaks are indexed to the layered  $\alpha$ -Ti(HPO<sub>4</sub>)<sub>2</sub>•H<sub>2</sub>O phase (JCPDS: 44-0382) and its sites of peaks are consistent with the reported data<sup>27</sup>. The presence of strongest peak at 11.56° suggests their interlayer distance is 7.65 Å due to well-ordered structure  $\alpha$ -TiP<sup>28</sup>. It is noteworthy that the intensity of (002) at 11.56° is higher than that of the reported results, which suggests dominant crystal growth along the [001] direction. After calcination at 500 °C (shown in Figure 3a), it is evident that the interlayer distance is decreased to 7.09 Å. This can be attributed to the fact that the crystal H<sub>2</sub>O and HPO<sub>4</sub><sup>2-</sup> were unstable in the process of heating treatment.

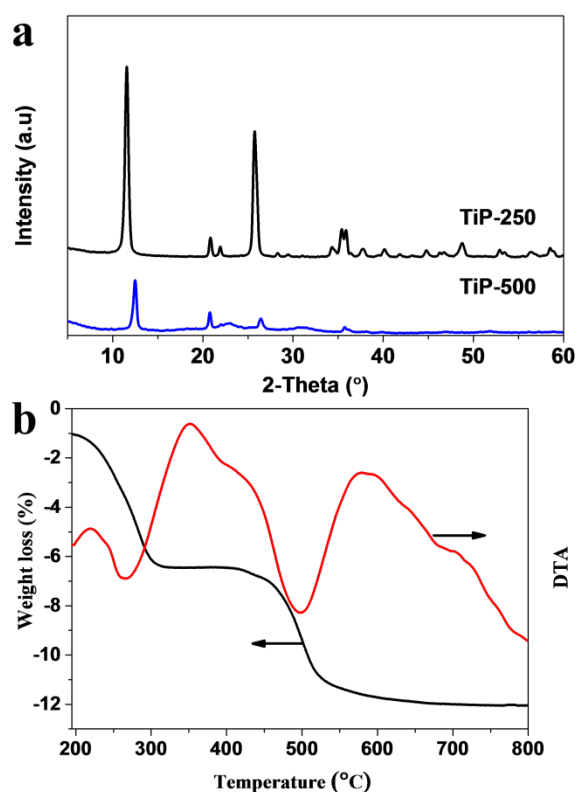


**Figure 3.** XRD patterns for the as-synthesized TiP obtained at 250 °C for 5 hours without calcination (a) and with calcination at 500 °C (b) TG and DTG curves for  $\alpha$ -TiP obtained at 250 °C for 5 hours.

The TG and DTG curves (Figure 3b) show that elongated  $\alpha$ -TiP nanoplates synthesized practically do only lose weight about 1% below 195 °C, which indicates that little or no physico-adsorption water exists in these compounds. Thermal decomposition of  $\alpha$ -TiP occurred in two steps. The first step starts at a temperature higher than room temperature and ends at 350 °C and then the other step ends at 710 °C, giving TiP<sub>2</sub>O<sub>7</sub>

as the final product, for the thermal degradation of  $\alpha$ -TiP takes place in the temperature range below 350 °C (6.44% weight loss) for crystal water and 350–710 °C (5.56% weight loss) for the chemical reaction of –OH. The total weight loss of the compounds is equal to 12.0% and the formula of  $\alpha$ -TiP could be represented as  $\alpha$ -Ti (HPO<sub>4</sub>)<sub>2</sub>•H<sub>2</sub>O in conformity with the XRD analysis.

The surface chemical composition of the as-prepared elongated hexagonal  $\alpha$ -TiP nanoplates at 250 °C for 5 hours was determined by XPS spectroscopy and the results are shown in Figure 4 and S3. An unsymmetrical O1s signal peak at 531.4 eV can be deconvoluted into three peaks at 531.2, 532.2, and 533.4 eV, respectively. The peak at 531.2 eV is the main assignment of O in Ti-O-P and P=O, the peak at 532.2 eV corresponds to O in P-O-H and the peak at 533.4 eV owns to O-C binding energy. The atom ratio of Ti-O-P/P=O : P-O-H is about 2:1 corresponding to the XPS data. The O1s of TiO<sub>2</sub> peaks at 530.1 eV and P in PO<sub>4</sub><sup>3-</sup> at 132.4 eV were not detected in XPS measurement, indicating that no Ti-O-Ti and PO<sub>4</sub><sup>3-</sup> existed in the powder.<sup>29</sup> The P2p peak, which should theoretically be an unresolved doublet with 2p<sub>1/2</sub> and 2p<sub>3/2</sub> components, was deconvoluted into two corresponding peaks at 134.2 and 133.4 eV respectively. The main component at 133.4 eV is attributed to the HPO<sub>4</sub><sup>2-</sup> group.<sup>30</sup> The XPS results support that the compositions of the powder have many –OH on the surface of  $\alpha$ -TiP. In Figure S3, Ti 2p<sub>1/2</sub> and Ti 2p<sub>3/2</sub> are present at binding energies of 465.8 eV and 460.1 eV, respectively, which aren't identical with the peaks at 464.8 eV and 459.0 eV, resulting from the Ti<sup>4+</sup> ions in tetrahedral environment.<sup>31,32</sup>

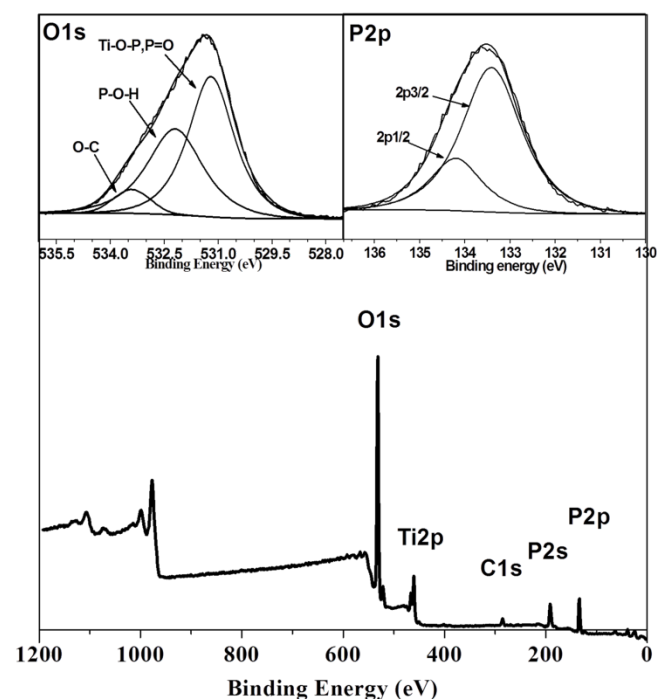


**Figure 4.** XPS spectra of  $\alpha$ -TiP obtained at 250 °C for 5 hours.

The FT-IR spectra of as-synthesized  $\alpha$ -TiP prepared at 250 °C for 5 hours were provided in Figure S4. The absorption peaks at 3557 and 3479  $\text{cm}^{-1}$  could be attributed to the symmetrical stretching band of the P-O-H group, and the broad peak in the region of 3000–3400  $\text{cm}^{-1}$  and the peak at 1260  $\text{cm}^{-1}$  correspond to the hydroxyl groups. The absorption band of resolved ( $\text{PO}_3$ ) asymmetry and ( $\text{PO}_3$ ) symmetry was observed in the region of 900–1300  $\text{cm}^{-1}$ , while the peak of the P-O-P bridge at 970  $\text{cm}^{-1}$  could hardly be observed, indicating that P in  $\alpha$ -TiP is in the form of  $\text{HPO}_4^{2-}$ .<sup>33</sup> After annealing at 500 °C, the symmetrical stretching band of the P-O-H group almost disappears and the absorption band in the region of 900–1300  $\text{cm}^{-1}$  is broader than the former, which is indicative of the formation of P-O-P bridge.<sup>31</sup> The exact peaks below 650  $\text{cm}^{-1}$  become weaker due to the change of phosphate groups framework.

According to the above results, the formation of  $\alpha$ -TiP is temperature-dependent. When the reaction temperature is above critical temperature (250 °C and 270 °C), the elongated hexagonal  $\alpha$ -TiP nanoplates were obtained, while the TiP nanosheets were formed as the reaction temperature is below the critical temperature (200 °C). As we know, the polarization and hydrogen bonds interaction are strongly dependent on temperature and can be adjusted continuously with temperature. At temperatures higher than critical temperature, hydrogen bonds become very weak and the number of monomers is big and that of the others oligomers such as three body and four body oligomers in the system is relatively small.<sup>34</sup> On the other hand, because the ionicity of reactants becomes higher with the temperature rising, the electrostatic interactions are still strong in the system. Herein we suggest that coordination bonding (mainly hydrogen bonds) and electrostatic interactions play a key role to the formation of elongated hexagonal  $\alpha$ -TiP nanoplates or nanosheets. Above 250 °C, the solvent strength became very weak and the weak hydrogen bonds make molecular kinetic energy become higher and higher with the increasing temperature.  $\text{Ti}^{4+}$  and other ions with high kinetic energy could directionally bind with electrostatic interaction on the  $\alpha$ -TiP facet. On this direction, there is comparatively stronger binding capability than other growth directions with coordination bonding. Therefore, the well-ordered elongated hexagonal  $\alpha$ -TiP nanoplates could be formed according to the possible crystal growth method that crystal growth is fast in the direction of length, which is confirmed by SEM and XRD analysis. However, the hydrogen-bonding interaction is still so strong below 200 °C that the  $\text{Ti}^{4+}$  and other ions have the same interaction with the facets in 2D orientation, because the ions do not have enough free energy to choose the facets to form elongated  $\alpha$ -TiP nanoplates. In short, the special properties of supercritical ethanol make the well-ordered elongated hexagonal  $\alpha$ -TiP nanoplates synthesized successfully.

## Conclusions

In summary, the single-crystal elongated hexagonal  $\alpha$ -TiP nanoplates have been successfully prepared in supercritical

ethanol with a template-free method. According to regulating the reaction conditions, the sizes of elongated hexagonal  $\alpha$ -TiP nanoplates could be controlled from 7 to 22  $\mu\text{m}$  in length. The elongated  $\alpha$ -TiP nanoplates may have interesting properties as single-crystal and well-structured materials. Additionally, this new synthesis route should be applicable to the synthesis of a variety of metal phosphates with controllable 2D nanostructures.

## Acknowledgments

This research was supported by Natural Science Foundation of China (21303038), Hefei University of Technology start-up grant (407037069).

## Notes and references

<sup>a</sup> Future Energy Laboratory, School of Materials Science and Engineering, Hefei University of Technology, Tunxi Road No.193 Hefei, Anhui, 230009, China E-mail: liujh@hfut.edu.cn.

<sup>b</sup> School of Chemistry and Chemical Engineering, Hefei University of Technology, Tunxi Road No.193 Hefei, Anhui, 230009, China

- J. M. Desimone, E. E. Maury, Y. Z. Menciloglu, J. B. McClain, T. J. Romack and J. R. Combes, *Science*, 1994, 265, 356-359.
- J. H. Liu, S. Q. Cheng, J. L. Zhang, X. Y. Feng, X. G. Fu and B. X. Han, *Angew. Chem. Int. Ed.*, 2007, 46, 3313-3315.
- A. A. Peterson, F. Vogel, R. P. Lachance, M. Froling, M. J. Antal and J. W. Tester, *Energy Environ. Sci.*, 2008, 1, 32-65.
- H. Weingartner and E. U. Franck, *Angew. Chem. Int. Ed.*, 2005, 44, 2672-2692.
- P. Lalanne, J. M. Andanson, J. C. Soetens, T. Tassaing, Y. Danten and M. Besnard, *J. Phys. Chem. A*, 2004, 108, 3902-3909.
- G. M. An, W. H. Ma, Z. Y. Sun, Z. M. Liu, B. X. Han, S. D. Miao, Z. J. Miao and K. L. Ding, *Carbon*, 2007, 45, 1795-1801.
- C. Slostowski, S. Marre, O. Babo, T. Toupance and C. Aymonier, *Langmuir*, 2014, 30, 5965-5972.
- M. Seo, D. Yoon, K. S. Hwang, J. W. Kang and J. Kim, *Carbon*, 2013, 64, 207-218.
- J. H. Liu, X. F. Wei, Y. L. Yu, J. L. Song, X. Wang, A. Li, X. W. Liu and W. Q. Deng, *Chem. Commun.*, 2010, 46, 1670-1672.
- J. H. Liu, J. L. Zhang, S. Q. Cheng, Z. M. Liu and B. X. Han, *Small*, 2008, 4, 1976-1979.
- N. Biswal, D. P. Das, S. Martha and K. M. Parida, *Int. J. Hydrogen Energy*, 2011, 36, 13452-13460.
- D. P. Das and K. M. Parida, *Appl. Catal. A Gen.*, 2007, 324, 1-8.
- L. N. Feng, J. Peng, Y. D. Zhu, L. P. Jiang and J. J. Zhu, *Chem. Commun.*, 2012, 48, 4474-4476.
- L.-N. Feng, Z.-P. Bian, J. Peng, F. Jiang, G.-H. Yang, Y.-D. Zhu, D. Yang, L.-P. Jiang and J.-J. Zhu, *Anal. Chem.*, 2012, 84, 7810-7815.
- A. Bhaumik and S. Inagaki, *J. Am. Chem. Soc.*, 2001, 123, 691-696.
- A. A. Khan, U. Baig and M. Khalid, *J. Hazard. Mater.*, 2011, 186, 2037-2042.
- J. Peng, L. N. Feng, Z. J. Ren, L. P. Jiang and J. J. Zhu, *Small*, 2011, 7, 2921-2928.
- S. Bruque, M. A. G. Aranda, E. R. Losilla, P. Olivera-Pastor and P. Maireles-Torres, *Inorg. Chem.*, 1995, 34, 893-899.

19. A. I. Bortun, S. A. Khainakov, L. N. Bortun, D. M. Poojary, J. Rodriguez, J. R. Garcia and A. Clearfield, *Chem. Mater.*, 1997, 9, 1805-1811.
20. M. Yada, Y. Inoue, A. Sakamoto, T. Torikai and T. Watari, *ACS Appl. Mater. Inter.*, 2014, 6, 7695-7704.
21. C. Serre, C. Lorentz, F. Taulelle and G. Férey, *Chem. Mater.*, 2003, 15, 2328-2337.
22. Z. L. Yin, Y. Sakamoto, J. H. Yu, S. X. Sun, O. Terasaki and R. R. Xu, *J. Am. Chem. Soc.*, 2004, 126, 8882-8883.
23. N. Biswal, S. Martha, U. Subudhi and K. Parida, *Ind. Eng. Chem. Res.*, 2011, 50, 9479-9486.
24. L. R. Cumba, U. D. Bicalho and D. R. do Carmo, *Int. J. Electrochem. Sci.*, 2012, 7, 4465-4478.
25. L. Mafrá, J. Rocha, C. Fernandez, G. R. Castro, S. Garcia-Granda, A. Espina, S. A. Khainakov and J. R. Garcia, *Chem. Mater.*, 2008, 20, 3944-3953.
26. K. Sarkar, M. Nandi and A. Bhaumik, *Appl. Catal. A Gen.*, 2008, 343, 55-61.
27. A. N. Christensen, E. K. Andersen, I. G. K. Andersen, G. Alberti, M. Nielsen and M. S. Lehmann, *Acta Chem. Scand.*, 1990, 44, 865-872.
28. A. Espina, J. R. García, J. M. Guil, E. Jaimez, J. B. Parra and J. Rodríguez, *J. Phys. Chem. B*, 1998, 102, 1713-1716.
29. G. Moretti, A. M. Salvi, M. R. Guascito and F. Langerame, *Surf. Interf. Anal.*, 2004, 36, 1402-1412.
30. C. Viornerly, Y. Chevolot, D. Léonard, B.-O. Aronsson, P. Péchy, H. J. Mathieu, P. Descouts and M. Grätzel, *Langmuir*, 2002, 18, 2582-2589.
31. T. Z. Ren, Z. Y. Yuan, A. Azioune, J. J. Pireaux and B. L. Su, *Langmuir*, 2006, 22, 3886-3894.
32. A. A. S. Alfaya, Y. Gushikem and S. C. de Castro, *Chem. Mater.*, 1998, 10, 909-913.
33. B. B. Sahu and K. Parida, *J. Colloid Interf. Sci.*, 2002, 248, 221-230.
34. D. Dellis, M. Chalaris and J. Samios, *J. Phys. Chem. B*, 2005, 109, 18575-18590.